CHAPTER IV
RESULTS AND DISCUSSION

In this chapter, the properties and the catalytic activity results of unmodified and modified HZSM-5 were illustrated and discussed. Moreover, the relations of catalytic properties and catalytic activity were explored in more detail to a better understanding of the prepared catalysts on methane dehydrogenation and coupling reactions.

4.1 Catalyst Characterization

To understand the property-reactivity relations of the catalysts prepared by polyol mediate process pertaining to catalytic performance in ethylene selectivity and methane conversion, all prepared catalysts were characterized by various techniques including catalyst composition, surface area, pore volume, acidity, reducibility as well as the amount of coke formation.

4.1.1 X-ray Diffraction (XRD)

Before the reduction step, all prepared catalysts were investigated for the particle size of NiO by XRD technique. The particle size of NiO was investigated in the region of the diffraction angle 2θ between 5 and 70° as shown in Figure 4.1. The characteristic XRD peaks corresponding to NiO is 37.44, 43.47 and 63.20 (2θ). However, these peaks were not clearly observed for all loaded catalysts. This can be suggested that the nickel was loaded with very small amount (Vitale *et al.*, 2013). Nevertheless, the difference of intensity between HZSM-5 and different Ni/HZSM-5 is observed. It can be observed that the intensity of 3%Ni/HZSM-5 decreased from 1%/HZSM-5 and unmodified HZSM-5 respectively. These results are the same trend as 3%Ni/HZSM-5 (HF) which the intensity is lower than 1%Ni/HZSM-5 (HF) and HZSM-5 (HF) respectively. This is probably due to a defect in crystallinity caused by the presence of the amount of Ni loading.
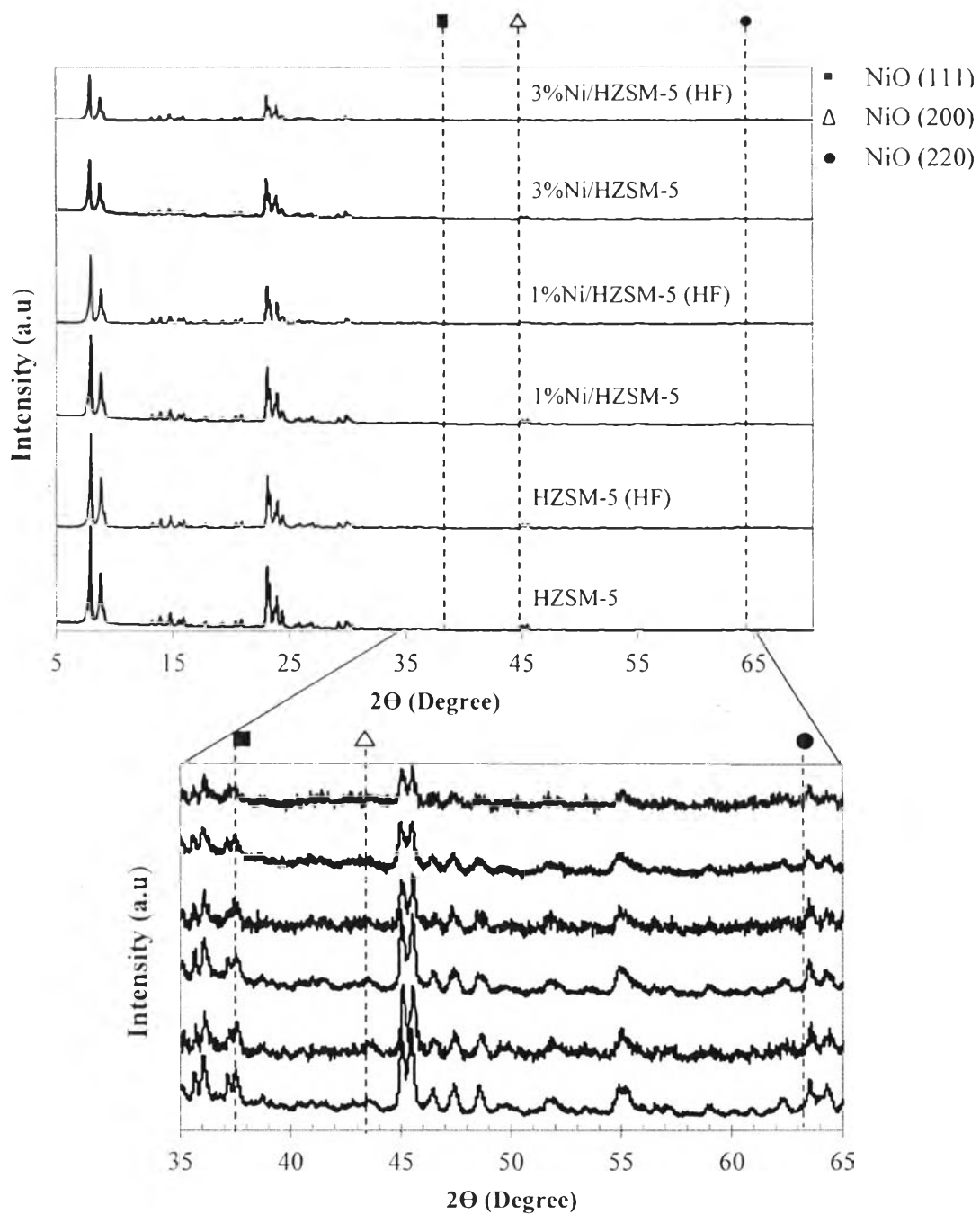
Figure 4.1 XRD patterns of the prepared catalysts.

4.1.2 X-ray fluorescence spectroscopy (XRF)

The result of elementals analysis from XRF measurements of all prepared catalysts were listed in Table 4.1.

Table 4.1 Chemical composition of prepared catalysts

Catalysts	Chemical composition	
	Si/Al mole ratio	Ni (wt%)
HZSM-5	23.8	-
1%Ni/HZSM-5	23.7	1.04
3%Ni/HZSM-5	23.5	2.81
HZSM-5 (HF)	27.8	-
1%Ni/HZSM-5 (HF)	26.0	0.92
3%Ni/HZSM-5 (HF)	25.4	2.92

To investigate the composition of the prepared catalysts, XRF technique was employed to determine the Si/Al ratio and the amount of Ni loading which would affect the dehydrogenation and coupling reaction. According to the results of Si/Al ratio in Table 4.1, the effect of Ni loading and the effect of dealumination using hydrofluoric acid are somewhat noticeable. In case of the effect of Ni loading, it was observed that the Si/Al ratio of HZSM-5 was not significantly changed as the amount of Ni loading was increased. This might be suggested that the amount of Ni loading of these catalysts is too small to affect the Si/Al ratio of their parent HZSM-5. On the contrary, the Si/Al ratio of HZSM-5 catalysts was affected by dealumination. These results were clearly observed in Table 4.1 which the HZSM-5 (HF) illustrated higher Si/Al ratio than those of untreated HZSM-5. This probably due to HF aqueous leached the partial aluminium in HZSM-5 framework. Thus, the acid sites probably were removed. It corresponded to hydroflorinated HZSM-5 which was treated by HF solution in order to mitigate or eliminated the Brönsted acid sites located on external surface of HZSM-5(Aboul-Gheit *et al.*, 2014). This would provide inactivated acid site on external surface resulting in decrease coke formation and enhance the product selectivity (Bhat *et al.*, 1996). Besides the effect of HF dealumination on the Si/Al ratio, it also effects on Ni dispersion as shown in Table 4.3. The percentage of metal dispersion of 1%Ni/HZSM-5, 1%Ni/HZSM-5 (HF), 3%Ni/HZSM-5 and 3%Ni/HZSM-5 (HF) are 5.12, 5.34, 1.43, and 1.39 respectively.

From these results. it can be observed that hydroflurination slightly enhanced the dispersion of low loading of Ni in the zeolites corresponding to (Aboul-Gheit *et al.*, 2010).

4.1.3 Scanning Electron Microscopy (SEM)

To understand the morphology of the catalysts, SEM was employed to investigate the changing of HZSM-5 compared to 1%Ni/HZSM-5 before reaction testing as shown in Figures 4.2 and 4.3. Moreover, 1%Ni/HZSM-5 after reaction testing at various temperatures was also observed and illustrated in Figures 4.4 and 4.5. Interestingly, the structure of fresh 1%Ni/HZSM-5 is changed after reaction testing at 750 °C and 800 °C. At reaction temperature 750 °C, the 1%Ni/HZSM-5 structure slightly changed and the agglomeration of particle was observed. The agglomeration of particle was clearly observed when increased the reaction temperature. This result would decrease in both conversion and selectivity to ethylene product due to loss of active sites.
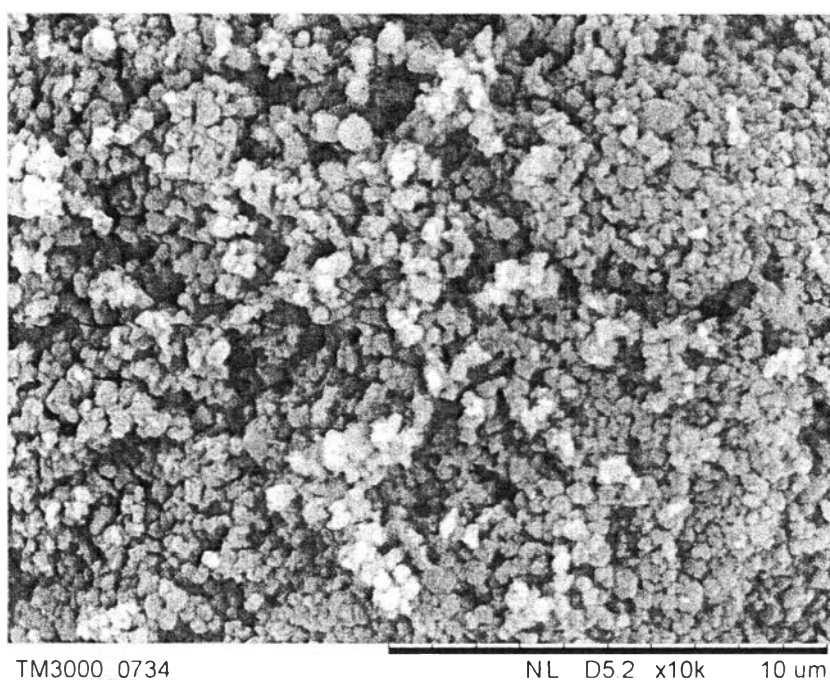

TM3000_0734   NL   D5.2   x10k   10 um

Figure 4.2 SEM image of unmodified HZSM-5.
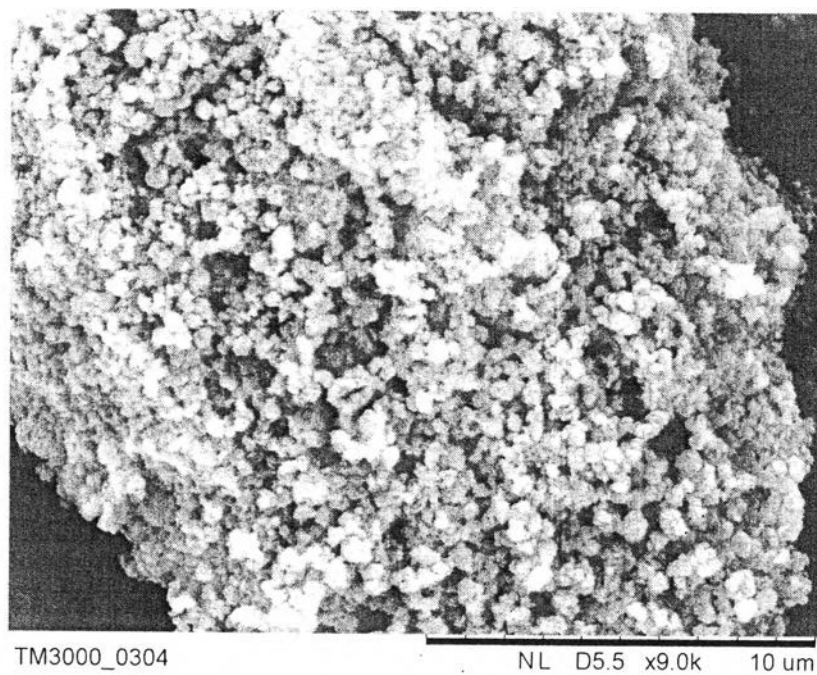
Figure 4.3 SEM image of fresh 1%Ni/HZSM-5.
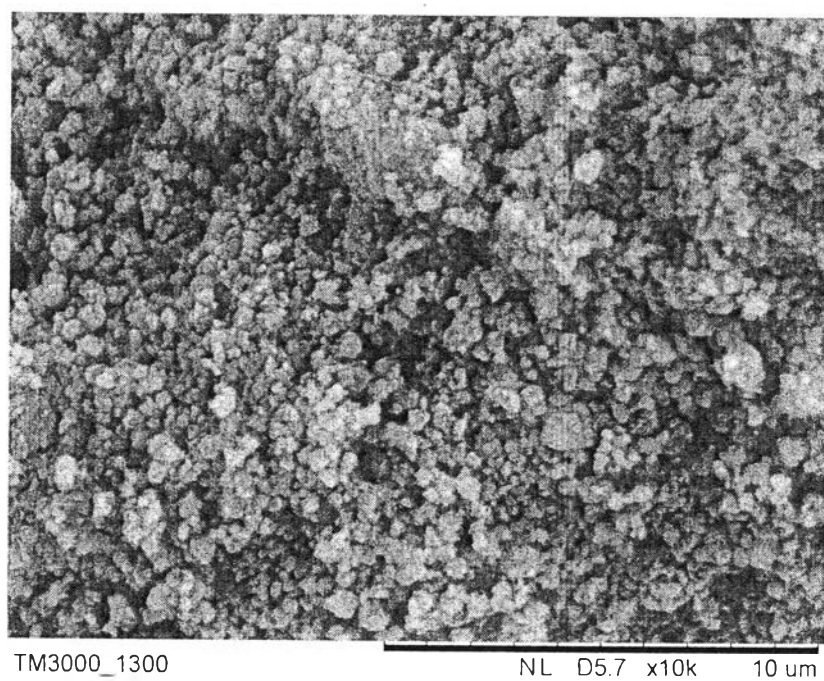
Figure 4.4 SEM image of the spent 1%Ni/HZSM-5 at reaction temperature 750 °C.
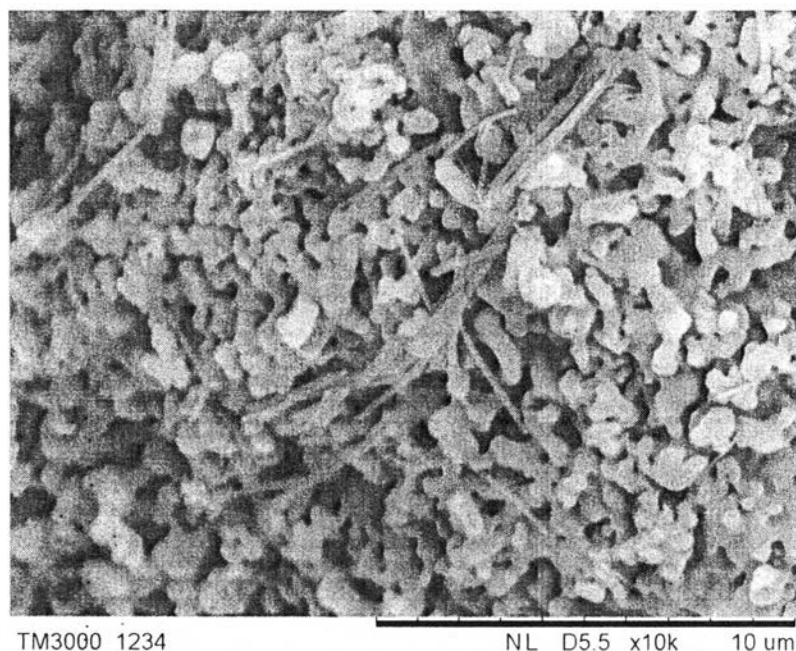
TM3000_1234   NL D5.5 x10k   10 um

Figure 4.5 SEM image of the spent 1%Ni/HZSM-5 at reaction temperature 800 °C.

4.1.4 Surface Area Measurements

The surface properties of catalysts were determined by N_2 adsorption-desorption method. The BET areas of the catalyst studied are summarized in Table 4.2. In cases of the parent HZSM-5 and the modified HZSM-5 (HF), the surface area of HZSM-5 (HF) (390m^2/g) was slightly higher than that of HZSM-5 (384 m^2/g). Moreover, all Ni loading supported on HZSM-5 (HF) catalysts which the total surface area is in the range of 314-376 m^2/g also exhibited higher total surface area than all Ni/HZSM-5 (273-332 m^2/g). This result probably affected by the effect of hydrofluorination which the surface area of HZSM-5 (HF) was improved by leaching out Al in HZSM-5 frame work. For both HZSM-5 and HZSM-5 (HF) with different Ni loading, the BET surface areas decreased with increasing Ni loading. This result could be attributed to the narrowing and blocking of nickel onto the pore opening and/or external surface. Moreover, micropore volume of HZSM-5 decreases from 0.1546 cm^3/g to 0.1214, and 0.0900 cm^3/g for 1% and 3%Ni/HZSM-5 respectively. This result are also observed in Ni incorporated on HZSM-5 (HF) which the micropore volume decreases from 0.1429 cm^3/g for to 0.1389 and 0.1075 cm^3/g for 1% and 3%Ni/HZSM-5 (HF) respectively. It is probably that Ni particle aggregation

at the mouth of the channels thus the micropore volume would decrease with more Ni loading (Vitale *et al.*, 2013). In case of total pore volume, it is clearly observed that HZSM-5 (HF) and 1%Ni/HZSM-5 (HF) significantly provide higher total pore volume than unmodified HZSM-5 and 1%Ni/HZSM-5 respectively. Noteworthy, this higher total pore volume and BET surface area of fluorinated HZSM-5 is mainly from the increase in the micropore. This result consists in (Feng *et al.*, 2010) which suggested that the fluorination treatment could create some secondary pore or dredge the channels of HZSM-5 zeolite.

Table 4.2 Textural properties of the catalysts studied

Catalyst	BET Surface area (m^2/g)	Total pore volume (cm^3/g)	Micropore volume* (cm^3/g)
HZSM-5	384	0.2092	0.1546
1%Ni/HZSM-5	332	0.2799	0.1214
3%Ni/HZSM-5	273	0.2841	0.0900
HZSM-5 (HF)	390	0.3685	0.1429
1%Ni/HZSM-5 (HF)	376	0.3196	0.1389
3%Ni/HZSM-5 (HF)	314	0.2819	0.1075

*Using t-plot method

Table 4.3 Metal dispersion of all loaded catalysts

Catalyst	Metal dispersion (%)
1%Ni/HZSM-5	5.12
3%Ni/HZSM-5	1.43
1%Ni/HZSM-5 (HF)	5.34
3%Ni/HZSM-5 (HF)	1.39

4.1.5 Temperature Programmed of Reduction of (Hydrogen-TPR)

A TPR technique was used to verify the temperature reduction of NiO into Ni^0 after calcination and investigate the reducibility of the prepared catalysts. The TPR profiles of all prepared catalysts are shown in Figure 4.6. No peak of H_2 consumption was observed for the parent HZSM-5and modified HZSM-5 (HF). both Ni/HZSM-5 and Ni/HZSM-5 (HF) had a broad peak of hydrogen consumption between 350-650 °C. This evidence confirms the presence of Ni in HZSM-5 and HZSM-5 (HF) support despite not detected by XRD technique. This result suggests that these catalysts had NiO species in their structure and it would be transformed into Ni metallic form at this temperature. Moreover, the reducibility of catalyst at low temperature about 400 to 600 °C corresponded to Ni nanoparticle located outside the external surface of HZSM-5. (Sarkar *et al.*, 2012). Additionally, 1%Ni/HZSM-5 and 3%Ni/HZSM-5 illustrate the broad peaks of hydrogen consumption at a higher temperature than 1%Ni/HZSM-5 (HF) and 3%Ni/HZSM-5 (HF) respectively. This result indicated that the NiO specie on unmodified HZSM-5 has higher strong interaction with the support than HZSM-5 (HF) (Moya *et al.*, 2011).
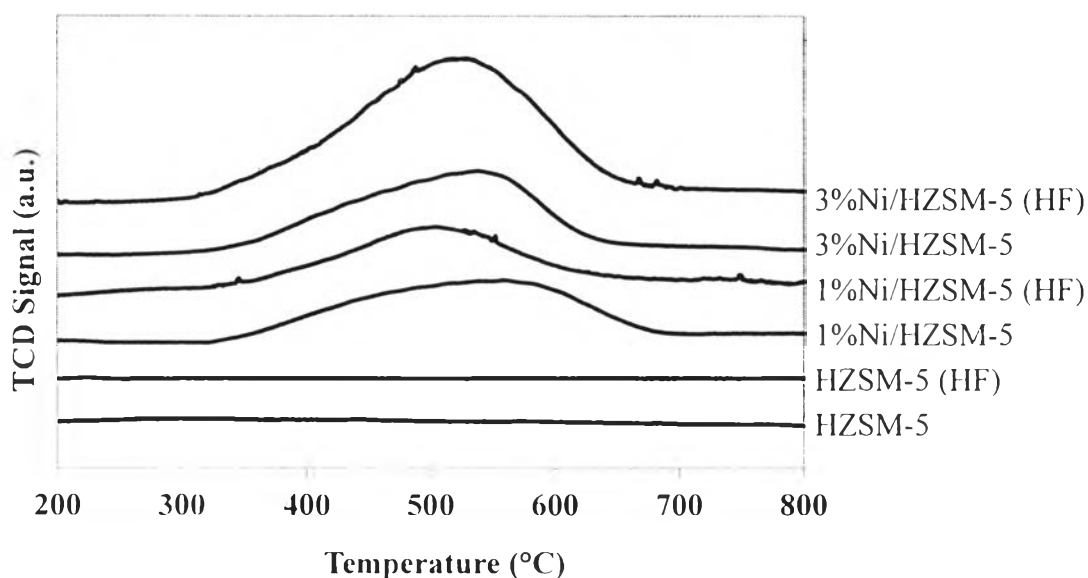

Figure 4.6 TPR profiles of the prepared catalysts.

4.1.6 Temperature Programmed Desorption of Isopropylamine (IPA-TPD)

IPA-TPD was used to investigate the Brönsted acid sites which play an important role in this reaction. It was already mentioned that Brönsted acid sites have a function for methane activation (Wang *et al.*, 1993). Due to the Brönsted acid sites would play an important role on methane conversion and ethylene selectivity.

IPA-TPD profiles of HZSM-5 and HZSM-5 (HF) are shown in Figure 4.7. exhibiting the amounts of Brönsted acid sites of both HZSM-5 and HZSM-5 (HF). The unmodified HZSM-5 has a slightly larger number of Brönsted acid sites than the HZSM-5 (HF). The decrease in Brönsted acid sites of HZSM-5 (HF) resulted from the dealumination by HF. This caused the alumina in framework to leach out as it is evidenced by an increase in Si/Al ratio. This effect causes the loss of strong acid by migrating into the channels of HZSM-5 zeolite and interacted with the bridging hydroxyl groups (Aboul-Gheit *et al.*, 2014). Besides the effect of hydrofluorination, the increase in Ni loading also effects on the decreasing in the amount of Brönsted acid sites which can be observed from both Ni incorporated on unmodified HZSM-5 and HZSM-5 (HF) as shown in Figures 4.8 and 4.9. This can be suggested that the Brönsted acid sites were covered by Ni particle which restricted the Brönsted acid sites exposing to interact with methane. And the decrease in Brönsted acid sites of prepared catalysts compared to HZSM-5 is summarized in Figure 4.10.
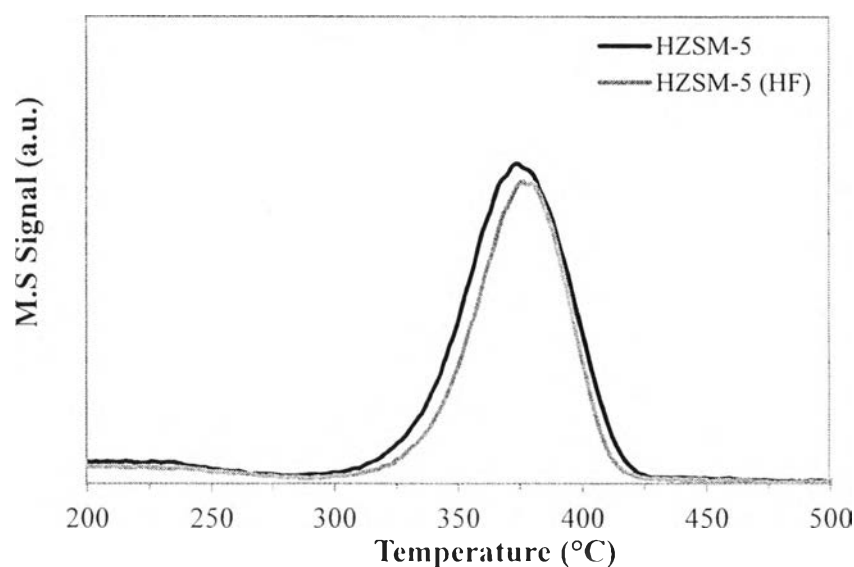
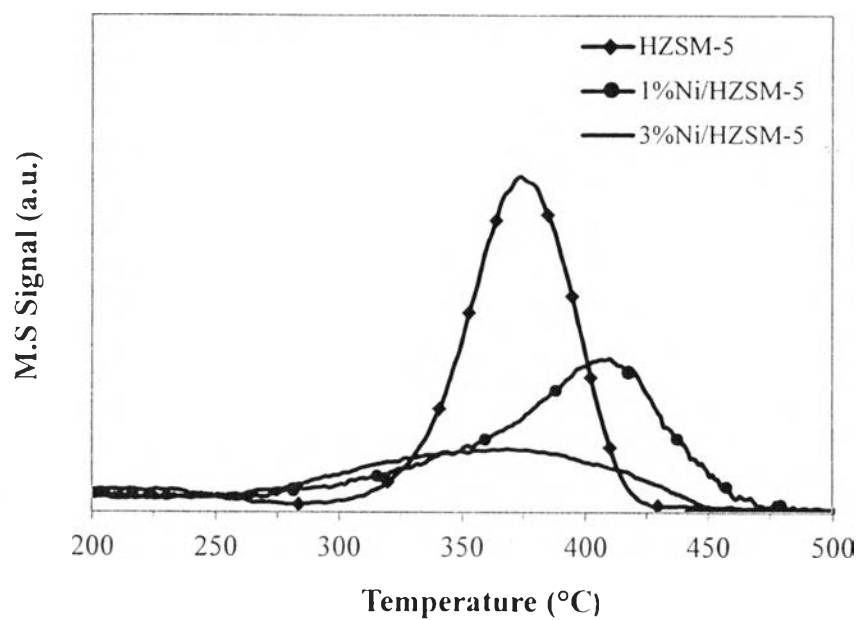

Figure 4.7 IPA-TPD profiles of HZSM-5 and HZSM-5 (HF).

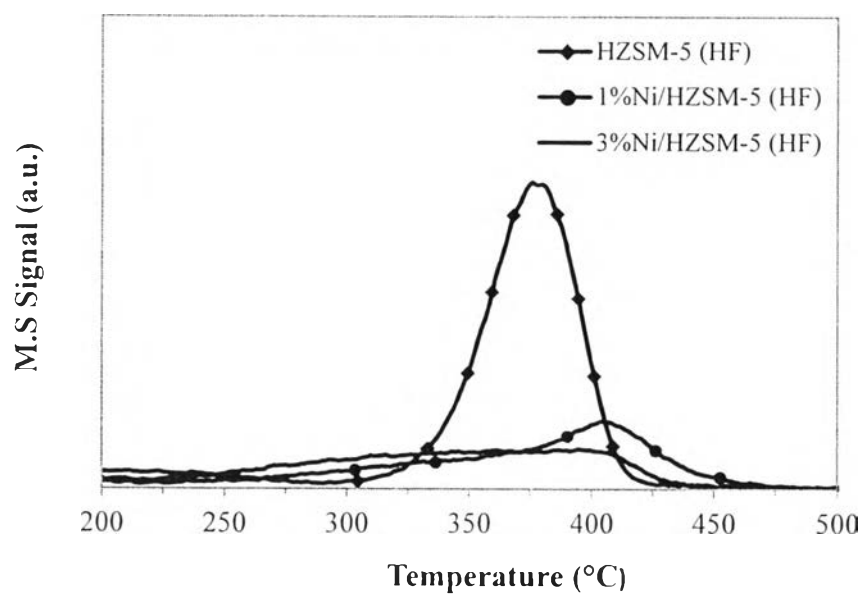**Figure 4.8** IPA-TPD profiles of HZSM-5 and Ni/HZSM-5.

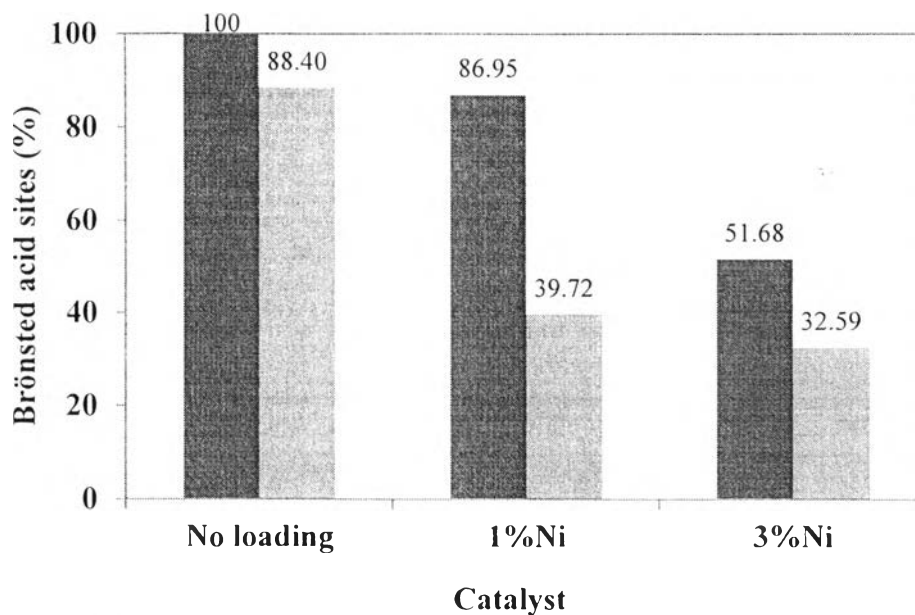Figure 4.9 IPA-TPD profiles of HZSM-5 (HF) and Ni/HZSM-5 (HF).

Figure 4.10 The relative amounts of the Brönsted acid sites in the absence and presence of Ni on (■) HZSM-5 and ( ) HZSM-5 (HF).

4.2 Catalytic Activity Testing for Methane Dehydrogenation and Coupling

To study the performance of all prepared catalysts for methane dehydrogenation and coupling reaction, the catalysts were tested for their catalytic activity under various conditions to obtain methane conversion and selectivity to ethylene. With this regard, the effects of Ni loading, reaction temperature, methane concentration, and hydrofluorination were investigated and discussed in the following sections.

4.2.1 Effect of Ni loading

Both HZSM-5 and HZSM-5 (HF) with different Ni loading were tested under given reaction conditions. The results are presented as follows:
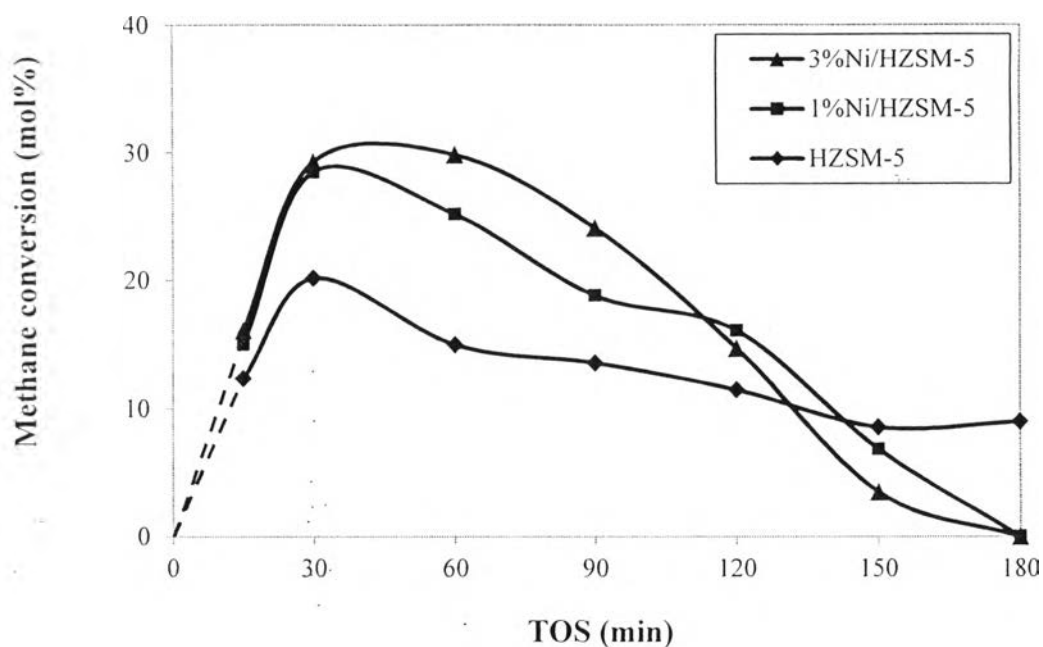
Figure 4.11 Methane conversion profiles for HZSM-5 and various Ni/HZSM-5 (750 °C, 20% CH_4 balanced in N_2, GHSV = 1500 ml/g/h).

Table 4.4 Gas product selectivity for HZSM-5 and various Ni/HZSM-5 (reaction temperature 750 °C, 20% CH_4, GHSV = 1500 ml/g/h)

Catalyst	Gas product	Gas product selectivity (mol.%) at						
		TOS (min)						
		15	30	60	90	120	150	180
HZSM-5	C_2H_4	N.D.	N.D.	N.D.	N.D.	N.D.	N.D.	N.D.
	C_3H_6	N.D.	N.D.	N.D.	N.D.	N.D.	N.D.	N.D.
1%Ni/	C_2H_4	N.D.	N.D.	43.12	31.03	10.63	12.91	N.D.
HZSM-5	C_3H_6	N.D.	100.00	56.88	68.97	89.37	87.09	N.D.
3%Ni/	C_2H_4	N.D.	N.D.	N.D.	N.D.	N.D.	N.D.	N.D.
HZSM-5	C_3H_6	N.D.	100.00	100.00	100.00	100.00	N.D.	N.D.

Note: N.D. = Not Detected

From Figure 4.11. all catalysts exhibit the ability for methane dehydrogenation reaction which can be seen from methane conversion. However, the presence of Ni on HZSM-5 catalysts showed higher methane conversion than unmodified HZSM-5. It can be attributed to the ability of dehydrogenation of Ni. In addition. increasing Ni loading from 1% to 3% slightly enhances the methane conversion for 120 min TOS then methane conversion of 3% rapidly decrease than 1%Ni. This can be suggested that more Ni loading generate more coke than small loading one which cause the Ni sites are covered by carbonaceous species resulting in decrease the performance of this catalyst. The coke formation is shown in Table 4.8.

Table 4.4 displays the selectivity of gas products including ethylene and propylene. It is noticeable that 1%Ni/HZSM-5 provides the highest selectivity to ethylene 43.12 % at 60 min TOS then the selectivity slightly drops and it cannot be observed after 150 min. Whereas, the propylene is more generated with time. This can be attributed to ethylene is an intermediate in this reaction then it further transforms to higher hydrocarbons on the acid sites corresponding to (Baba *et al.*, 2002). This suggested two new routes for light olefin synthesis. These routes illustrate that methane could be converted to propylene as reactions 4.1 and 4.2.

$$CH_4 + CH_2=CH_2 \rightarrow CH_3CH=CH_2 + H_2 \tag{4.1}$$

$$3CH_2=CH_2 \rightarrow 2CH_3CH=CH_2 \tag{4.2}$$

If methane could be converted into propylene in the presence of ethylene and using metal cation-exchanged it will provide propylene as a main product.

With 3%Ni/HZSM-5, it provides the selectivity of propylene more than 1%Ni/HZSM-5 as shown in Table 4.4.This probably was because of catalyst deactivation from coke formation generated by high Ni loading. This coke would inhibit methane decomposition leads to decrease ethylene production which was further used to propylene production as shown in reaction 4.2.

4.2.2 Effect of Hydrofluorination

According to the study of H-ZSM-5 hydrofluorination in non-oxidative conversion of natural gas (Aboul-Gheit *et al.*, 2014), the effect of hydrofluorination was studied to improve the selectivity of ethylene. In terms of methane conversion, HZSM-5 (HF) and loaded HZSM-5 (HF) exhibited slightly higher catalytic activity for methane conversion than the HZSM-5 and loaded HZSM-5 as shown in Figures 4.12, 4.13, and Figure 4.14. This probably due to the amount of Brönsted acid sites was decreased by hydrofluorination consisted with TPD-PA results. This is the main reason that hydrofluorination enhanced activity and the prolonged lifetime of the catalyst(Aboul-Gheit *et al.*, 2014). For selectivity to ethylene from Table 4.6, both of loaded HZSM-5 (HF) similarly provides high selectivity to ethylene compared to 1%Ni loading and low selectivity to ethylene when Ni was increased to 3%Ni.
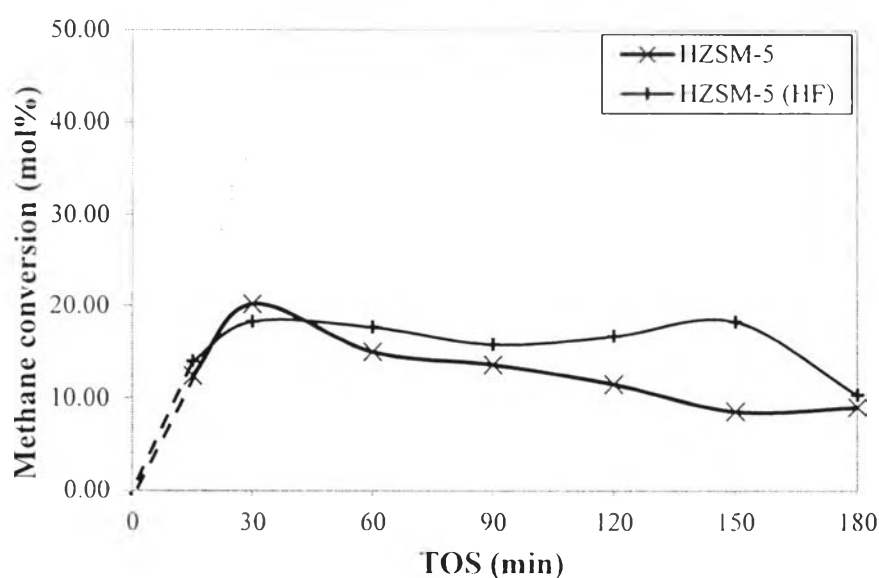

Figure 4.12 Methane conversion profiles over HZSM-5 and HZSM-5 (HF) (750 °C, 20% CH₄ balanced in N₂, GHSV = 1500 ml/g/h).
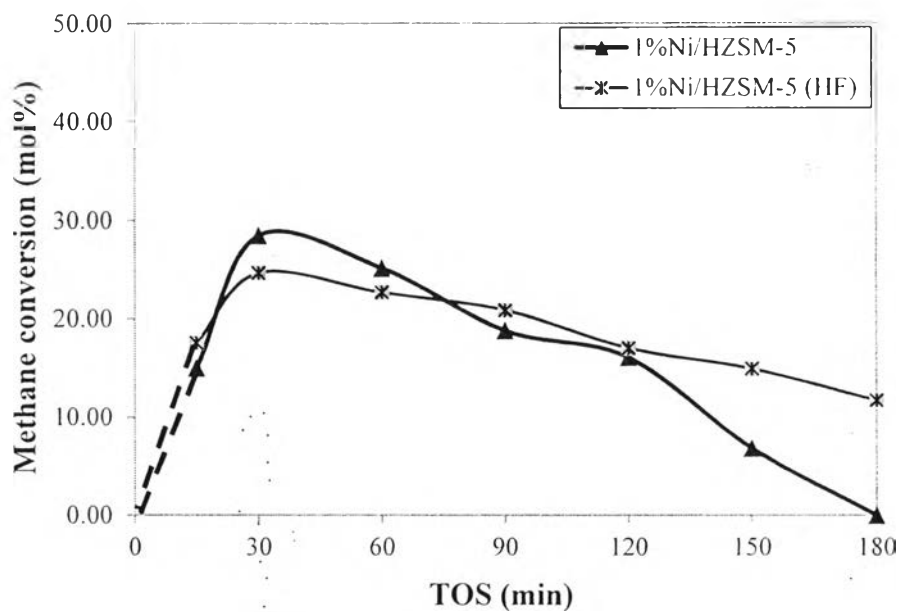
Figure 4.13 Methane conversion profiles over 1%Ni/HZSM-5 and 1%Ni/HZSM-5 (HF) (750 °C, 20% CH_4 balanced in N_2, GHSV = 1500 ml/g/h).
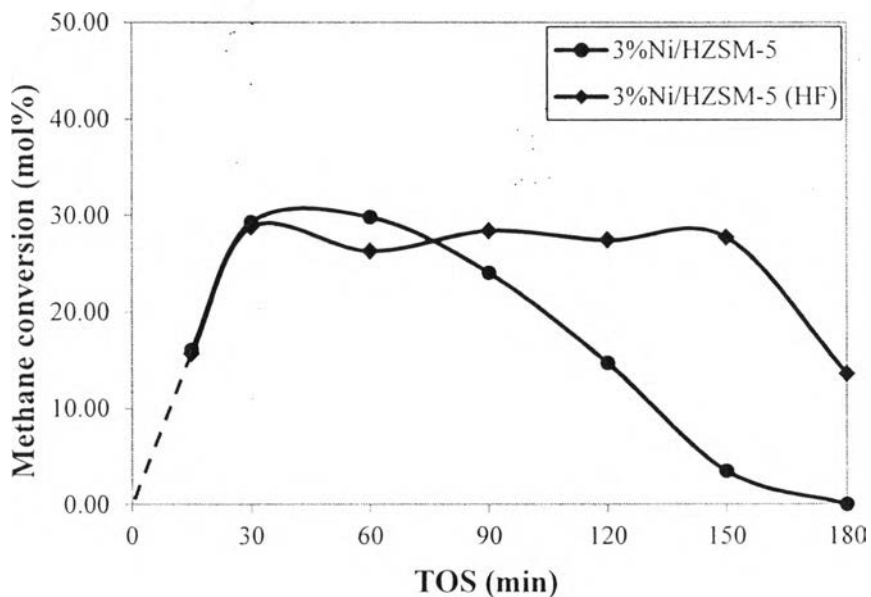

Figure 4.14 Methane conversion profiles over 3%Ni/HZSM-5 and 3%Ni/HZSM-5 (HF) (750 °C, 20% CH_4 balanced in N_2, GHSV = 1500 ml/g/h).

Table 4.5 Gas product selectivity for unloaded HZSM-5 (HF) and loaded HZSM-5 (HF) (reaction temperature 750 °C, 20% methane, GHSV = 1500 ml/g/h)

Catalyst	Gas product	Gas product selectivity (mol.%)						
		TOS (min)						
		15	30	60	90	120	150	180
HZSM-5	C_2H_4	N.D.	N.D.	N.D.	N.D.	N.D.	N.D.	N.D.
(HF)	C_3H_6	N.D.	N.D.	N.D.	N.D.	N.D.	N.D.	N.D.
1%Ni/	C_2H_4	N.D.	N.D.	19.41	22.53	27.85	27.86	29.51
HZSM-5 (HF)	C_3H_6	N.D.	N.D.	80.59	77.47	72.15	72.14	70.49
3%Ni/	C_2H_4	N.D.	N.D.	N.D.	N.D.	N.D.	N.D.	N.D.
HZSM-5 (HF)	C_3H_6	N.D.	100.00	100.00	100.00	100.00	100.00	N.D.

4.2.3 <u>Effect of Reaction Temperature</u>

It is well knows that dehydrogenation reaction of methane is an endothermic reaction. Therefore, higher temperature is required to enhance this reaction. According to the result of methane conversion as shown in Figure 4.15, increase in reaction temperature to 800 °C significantly improves methane conversion through course of reaction compared to 750 °C.

Moreover, increase in reaction temperature can also increase ethylene selectivity and the highest ethylene selectivity is 100% attained at 1%Ni/HZSM-5 when the reaction was carried out at 800 °C. However, high temperature can reduce catalytic activity because the nickel particles will agglutinate and grow large in high temperature (Gao *et al.*, 2001) which can be observed form SEM image in Figure 4.5.
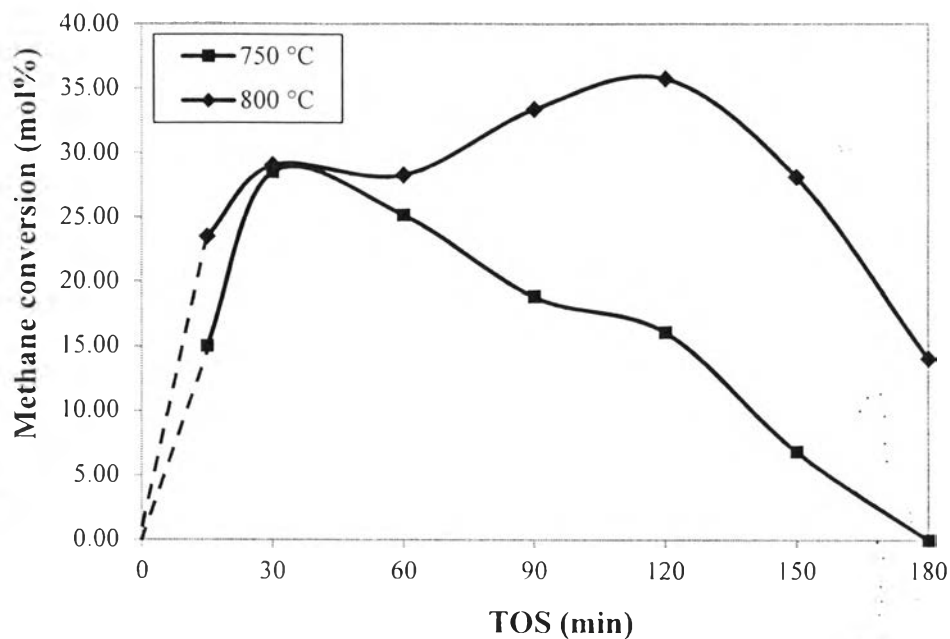
Figure 4.15 Catalytic activity testing over 1%Ni/HZSM-5 (750 and 800 °C, at 20% CH_4 balanced in N_2, GHSV = 1500 ml/g/h).

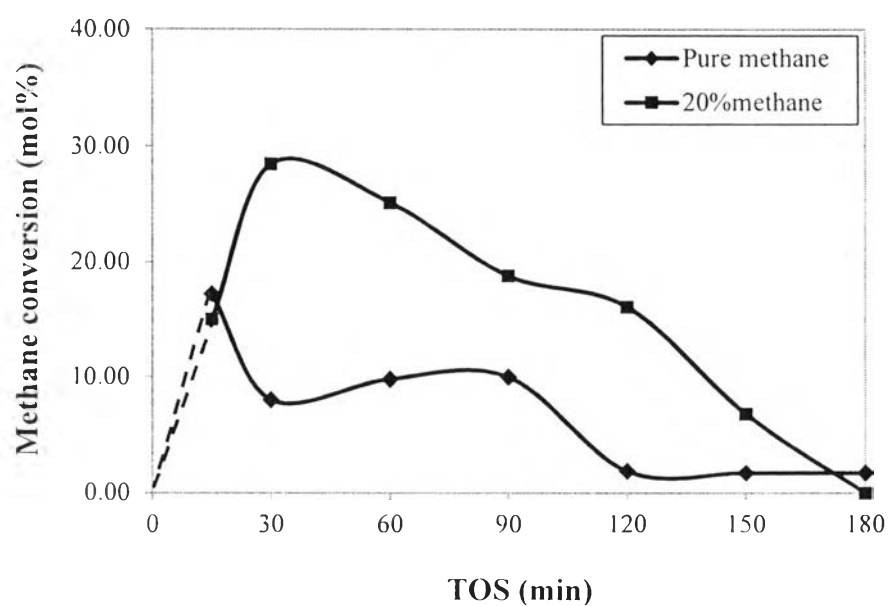### 4.2.4 Effect of Methane Concentration

Figure 4.16 Catalytic activity testing over 1%Ni/HZSM-5 for different CH_4 concentration at 750 °C, GHSV = 1500 ml/g/h.

To avoid high coke formation from using Ni as a catalyst, methane concentration was studied by varying methane in feed for 20% methane compare to pure methane. From Figure 4.15, it is noteworthy that 20% has high efficiency than using pure methane as a feed. In term of methane conversion, 20% methane illustrates higher methane conversion through course of reaction. Moreover, it can yield the ethylene product whereas no gas products were observed for using only methane as a feed. With TPO technique, the amount of coke formation is shown in Table 4.6 and the TPO profile is shown in Figure 4.17. This evidences that pure methane generates 4 times of coke compare to 20% methane feed. This can be suggested that high methane composition in feed accelerates the deactivation of catalyst by high coke formation resulting in low methane conversion.

Table 4.6 Coke formation of the catalyst at different methane concentration in feed

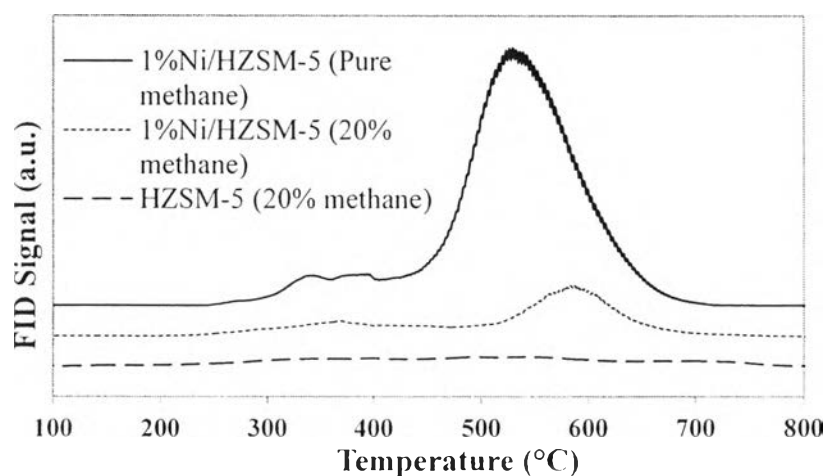| Catalyst	Methane concentration (mol %)	Coke formation (wt.%)
HZSM-5	20	0.11
1%Ni/HZSM-5	20	0.30
1%Ni/HZSM-5	100	1.23
3%Ni/HZSM-5	20	0.50

Figure 4.17 TPO profiles of the catalysts studied.